Atmospheric Environment 44 (2010) 858–866

Contents lists available at ScienceDirect

Atmospheric Environment

journal homepage: www.elsevier.com/locate/atmosenv

# Two extreme types of mixing of dust with urban aerosols observed in Kosa particles: 'After' mixing and 'on-the-way' mixing

Issei Suzuki[a], Yasuhito Igarashi[b], Yukiko Dokiya[c], Tasuku Akagi[d,*]

[a] Department of Earth and Planetary Sciences, Graduate School of Sciences, Kyushu University, 6-10-1 Hakozaki, Higashi-ku, Fukuoka 812-8581, Japan
[b] Meteorological Research Institute, 1-1 Nagamine, Tsukuba-shi, Ibaraki 305-0052, Japan
[c] Edogawa University, 474 Komaki, Nagareyama-shi, Chiba 270-0198, Japan
[d] Department of Earth and Planetary Sciences, Faculty of Sciences, Kyushu University, 6-10-1 Hakozaki, Higashi-ku, Fukuoka 812-8581, Japan

ARTICLE INFO

*Article history:*
Received 8 May 2009
Received in revised form
6 November 2009
Accepted 11 November 2009

*Keywords:*
Asian dust
$Ca^{2+}$
Background Kosa
$SO_4^{2-}$
$NH_4^+$

ABSTRACT

Besides well-known episodic Kosa during spring, high concentrations of $Ca^{2+}$ in aerosols were observed early in summer as well as in the semi-continuous data of the aerosols at the summit of Mt. Fuji. We further analysed the data to study the chemical characteristics of the high calcium event during early summer. The back trajectory analyses of the event indicated that Ca was transported from arid and semi-arid regions (e.g. the Taklamakan desert) through the westerly-dominated troposphere higher than the height of the summit of Fuji. The amount of $SO_4^{2-}$ was always equivalent to that of $NH_4^+$ unlike the case of the normal Kosa period where $SO_4^{2-}$ is in excess with respect to $NH_4^+$. This shows the 'after' mixing of unreacted $CaCO_3$ of Kosa origin with $(NH_4)_2SO_4$, which was only realized by the downward injection of Kosa particles from higher altitudes to the air masses of different origin. In the case of normal Kosa, the air bearing Kosa particles passed through the polluted area to absorb unneutralized acids ('on-the-way' mixing), whereas in the case of the Kosa-like phenomena in summer, the acids from the polluted area have been neutralized by $NH_4^+$ and become inactive before mixing with $CaCO_3$ ("after" mixing). We have simplified the chemistry of aerosols using their three major components, $Ca^{2+}$, $SO_4^{2-}$ and $NH_4^+$, and introduced a new triangle diagram with the three assumed end-members of $CaCO_3$, $CaSO_4$ and $(NH_4)_2SO_4$ to quantify the contribution of the 'after' mixing to the aerosols (AMI; 'after' mixing index). Based on the back trajectories of some high AMI cases, $CaCO_3$ in Kosa particles was transported through the middle troposphere (5000–7000 m) and descended to meet another air mass where $SO_4^{2-}$ had been already neutralized by $NH_3$.

## 1. Introduction

Dust events have a global impact on the climate and the ecosystem. An Asian dust phenomenon normally occurs in spring. Recently, researchers have performed various studies on the phenomenon, including lidar observation (Kai et al., 1988; Sakai et al., 2002), model simulations (Takemura et al., 2002; Tanaka et al., 2005), particle sampling and analysis (Okada and Kai, 1995; Kim and Park, 2001; Yabuki et al., 2002; Okada et al., 2005) and airplane sampling (Hatakeyama et al., 2004). Most studies were performed during the spring dust events. Iwasaka et al. (1988) detected a weak dust layer in summer using lidar observation. Asian dust was also discovered to be transported in summer only recently (Iwasaka et al., 2003, 2004; Matsuki et al., 2003; Kim et al., 2004; Watanabe, 2005). Matsuki et al. (2003) detected dust in summer as well as spring by airplane sampling and found that the dust was steadily transported on a small scale through the middle free troposphere (2–6 km). The back trajectory analyses of the dust suggested that it originated from the Taklimakan desert. Watanabe (2005) observed a high concentration of $Ca^{2+}$ in fog water at Mt. Norikura in summer and believed that it was due to Asian dust. Although a number of observations indicate the dust transport in summer, however, no intensive studies from chemistry viewpoint have been performed.

Aerosol sampling was performed over the course of a year at the summit of Mt. Fuji between 2001 and 2002 and the concentrations of major ions in the aerosols were determined (Suzuki et al., 2008). Some peaks in the Ca concentration were observed even in summer during the course of study (Suzuki et al., 2008). In this study, the data have been closely analysed to address the aerosol chemistry during summer and its transport mechanism.

---

* Corresponding author. Tel./fax: +81 92 642 4187.
*E-mail address:* akagi@geo.kyushu-u.ac.jp (T. Akagi).

1352-2310/$ – see front matter © 2009 Elsevier Ltd. All rights reserved.
doi:10.1016/j.atmosenv.2009.11.030

## 2. Experimental method

The sampling and analytical procedures have already been described in our earlier study (Suzuki et al., 2008). Here, we briefly restate them below.

### 2.1. Sampling site

Aerosol samples were collected at the Mt. Fuji Weather Station of the Japan Meteorological Agency (JMA), located at the highest hill of the summit (3776 m a.s.l. at 35.21°N, 138.43°E) (Fig. 1) on the west side of the crater (radius ca. 500 m). The influence due to vegetation and visitors is considered to be negligible based on the geographical position of the station (see Suzuki et al., 2008 for details).

### 2.2. Sampling method and measurement of water-soluble ionic species in aerosols

Aerosol samples were collected using a high volume sampler (HV-1000F, Sibata Scientific Technology Ltd., Japan, flow rate at ca. 700 L $\mathrm{min}^{-1}$). The sampling periods were between June 2001 and September 2002. Filters were renewed once every week from July till the beginning of March 2002, and then everyday until the middle of September (Suzuki et al., 2008). Filters were usually exchanged at around 9:00 a.m. in local time. Total volume of air, which passed through the filter for each run, was measured for the basis of the data. We used the one day sampling data from the middle of March till the beginning of September in this study.

The filters were cut and soaked in 20 mL of distilled water. Water-soluble ions were extracted from each of the cut filters by ultrasonification, and the concentrations of the main water-soluble ionic species were determined by ion chromatography. Details of the sampling method and measurement of the water-soluble ionic species were described in Suzuki et al. (2008).

### 2.3. Backward trajectory analysis

Isentropic backward trajectory analysis was performed using METEX, Meteorological Data Explorer (Center for Global Environmental Research, National Institute for Environmental Studies, Japan, URL: http://db.cger.nies.go.jp/metex/). The wind fields used in the analysis are from the data set of the European Centre for Medium-Range Weather Forecast (ECMWF), having time and spatial resolution of 6 h and 2.5°, respectively. The data set consists of winds, temperature, geopotential and other parameters on 15 absolute pressure levels (1000, 925, 850, 700, 500, 400, 300, 250, 200, 150, 100, 70, 50, 30 and 10 hPa) and on the surface (Zeng et al., 2003). Back trajectories during the 120 h before the middle of the sampling time were calculated.

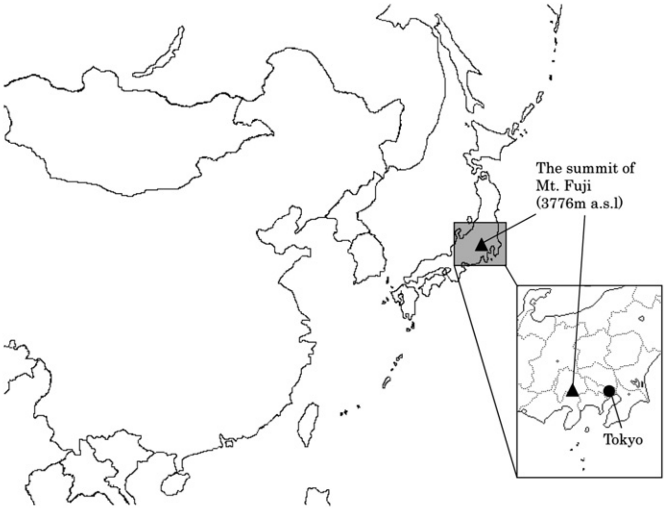

**Fig. 1.** Location of sampling site of Mt. Fuji.

## 3. Results and discussion

### 3.1. Kosa event at the summit of Mt. Fuji

$CaCO_3$ is one of the most representative components of desert and loess soils in China (Chang et al., 2000). Kosa particles are reported to contain $Ca^{2+}$ (Okada and Kai, 1995; Kim and Park, 2001; Yabuki et al., 2002; Okada et al., 2005) at concentrations as high as 2–6 weight % (Nishikawa et al., 1991), and the concentration of $Ca^{2+}$ in aerosols is a good indicator of Kosa particles. The concentrations of $Ca^{2+}$ in aerosols at the summit of Mt. Fuji from 11 March to 10 September are shown in Fig. 2.

From March to May, high concentrations of $Ca^{2+}$ were frequently observed. Kosa events are considered to be responsible for the peaks (Suzuki et al., 2008). The maximum concentration of $Ca^{2+}$ was 129.4 nmol $\mathrm{m}^{-3}$ during the first three months from March to May. From June to August, high concentrations of $Ca^{2+}$ still appeared very occasionally as on 4th July (81.7 nmol $\mathrm{m}^{-3}$) and 2nd June (36.6 nmol $\mathrm{m}^{-3}$). These peaks of Ca were also considered to originate from desert sand and loess like the Kosa events in spring. Similar Kosa-like phenomena were observed in summer and autumn at relatively higher altitudes in Japan (Matsuki et al., 2003; Watanabe, 2005).

In spring, the $NH_4^+/SO_4^{2-}$ equivalent ratio was much lower than unity and the concentration of $Ca^{2+}$ in aerosols was high, whereas the ratio was about 1.0 in summer, irrespective of concentrations of $Ca^{2+}$ (see Fig. 2). There seems to be a distinctive difference in aerosol chemistry between Kosa in spring and Kosa-like phenomena in summer, which will be discussed in detail in the following sections.

### 3.2. $Ca^{2+}$–$SO_4^{2-}$–$NH_4^+$ diagram

Fig. 3 shows the annual mean equivalent ratio of water-soluble components of aerosols. $Ca^{2+}$, $SO_4^{2-}$ and $NH_4^+$ accounted for 90.8% of the annual mean equivalent ratio. In order to visually show the seasonal variations of the aerosol chemistry related with Kosa particles, they are plotted in a triangle diagram of $Ca^{2+}$, $SO_4^{2-}$ and $NH_4^+$ (Figs. 4 and 5). We use the data where the sum of three ions constituted more than 85% of the total ions. This figure is arbitrarily

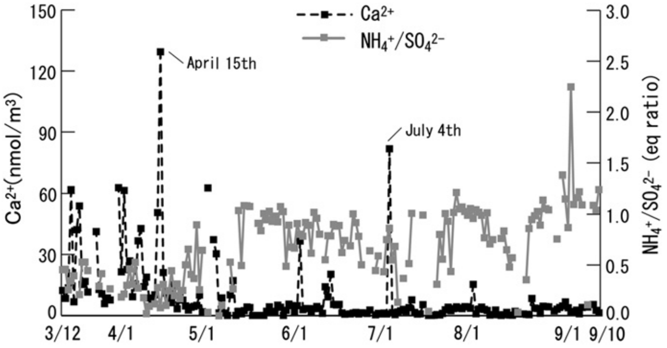

**Fig. 2.** Concentrations of $Ca^{2+}$ (nmol $\mathrm{m}^{-3}$) and $NH_4^+/SO_4^{2-}$ (ratio in equivalent) in aerosols at the summit of Mt. Fuji during the observation period: 11 March–10 September 2002.

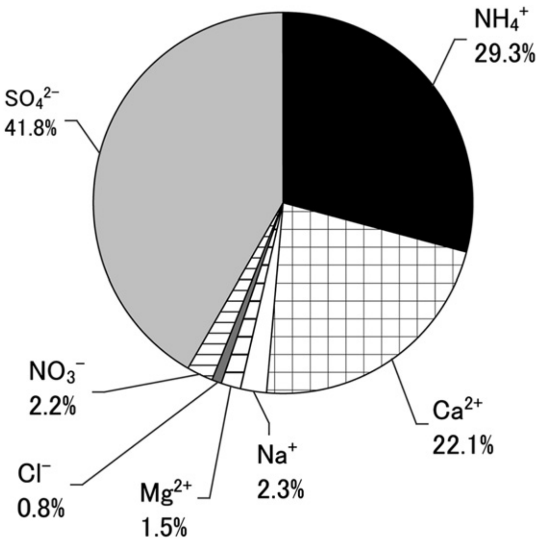

**Fig. 3.** Mean concentrations of water-soluble components of the aerosols collected from 11 March to 10 September 2002 (equivalent percentage).

chosen to attain a compromise between the number of data and its overall precision. The days account for 87% of the total number of samples.

Two of the three end-members are cations, and the solid line (Line 1) in Fig. 4 represents the state of ion balance of the three ion species. Because in most of the cases the balance is not met by the three ion species, it is necessary to introduce other ion species. The contributions of $NO_3^-$, $Mg^{2+}$, $Na^+$ and $Cl^-$ should be small because their sum constituted less than 15% of the total ions. We have to introduce $H^+$ in the case of cation deficiency and $CO_3^{2-}$ in the case of anion deficiency. Both of them were not measurable with the ion chromatography. The region under Line 1 corresponds to the state wherein $SO_4^{2-}$ is in excess over the sum of $Ca^{2+}$ and $NH_4^+$. We have to introduce $H^+$ to balance the excess anions, and therefore, we named this region the 'acid region'. The upper region above Line 1 corresponds to the state wherein $Ca^{2+}$ and $NH_4^+$ are in excess over $SO_4^{2-}$. As has been discussed in detail in our earlier study (Suzuki et al., 2008), carbonate ion has to be considered to compensate for the excess cations. When carbonate is assumed to be $CaCO_3$, the excess that can be explained by the carbonate is limited by Line 2. Therefore, we named the region sandwiched between lines 1 and 2 the 'carbonate region'. This assumption is reasonable as $CaCO_3$ is one of the major components of the Kosa particles. The region to the right of Line 2 corresponds to the state wherein the sum of $NH_4^+$ and $Ca^{2+}$ is in excess over the sum of $SO_4^{2-}$ and $CO_3^{2-}$. The scrutiny of the data revealed that $NO_3^-$ ion, which was not considered in the diagram, was responsible for the relatively small excess.

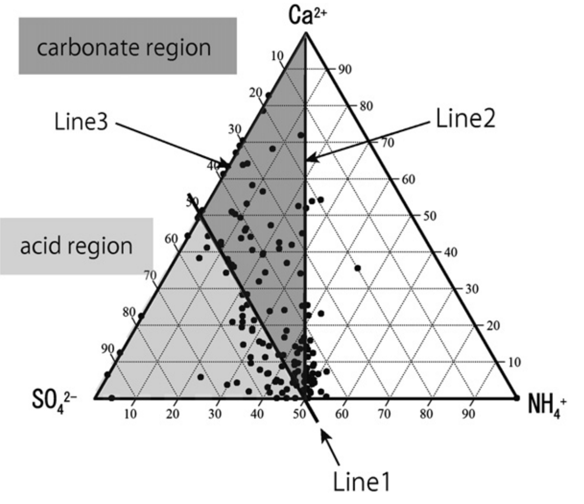

**Fig. 4.** Triangle diagram ($Ca^{2+}$–$SO_4^{2-}$–$NH_4^+$) of aerosols at the summit of Mt. Fuji.

The three lines are thus mixing lines between two of some typical chemical compounds supplied to the aerosols by the Kosa particles or existing originally in the aerosols themselves. Line 1 (Fig. 4) indicates the mixing of $(NH_4)_2SO_4$ and $CaSO_4$. The mixture of unreacted Ca ion ($CaCO_3$) and $(NH_4)_2SO_4$ lies on Line 2. Along the upper and lower half of Line 3, the mixture of $CaSO_4$ and unreacted Ca ($CaCO_3$) and that of $CaSO_4$ and unreacted $SO_4^{2-}$ ($H_2SO_4$) is plotted, respectively.

Fig. 5 shows the monthly triangle diagrams. In March, most of the data fell along Line 1, indicating that the aerosols were a mixture of $CaSO_4$ with $(NH_4)_2SO_4$. The greatest amount of Kosa particles was transported in April, most of the data for which were located in the region sandwiched between the upper half of Line 3 and the upper half of Line 1. This suggests that $Ca^{2+}$ occurred as $CaCO_3$ or $CaSO_4$. In fact, $CaCO_3$ and $CaSO_4$ were observed in the dust storm (Wang et al., 2005; Tsai and Chen, 2006; Suzuki et al., 2008).

Several research groups have suggested that $CaSO_4$ is produced by the reaction between polluted air and Kosa particles (Kim and Park, 2001; Yuan et al., 2006; Suzuki et al., 2008). The main source of $SO_4^{2-}$ is considered to be anthropogenic emissions of $SO_2$. It is likely that polluted air from industrial areas and air masses containing Kosa particles were mixed during the dust storms. The $SO_2$ gas is not stable under solar radiation and quite readily oxidized to $SO_4^{2-}$ ion in an aqueous phase or in a gaseous phase by OH radical oxidation with a half life as short as 15 h (Ito et al., 1986) to about one day (Berresheim et al., 1990). The reaction could be accelerated with the presence of mineral surfaces and $CaSO_4$ may form directly from the $SO_2$ adsorbed by Kosa particles (Li et al., 2006). The desert sand particles may contain $CaSO_4$ from the beginning. However, the molar ratio of $SO_4^{2-}$/Ca is as low as 0.001–0.04 (Nishikawa et al., 1991) and much lower than the ratio observed in this study. Most of the $Ca^{2+}$ in $CaCO_3$, therefore, might have reacted with $SO_4^{2-}$ or $SO_2$, and little of the $CaCO_3$ remained unreacted ('on-the-way' mixing).

On the other hand, from June to September, much of the data fell near Line 2, the mixing line of $(NH_4)_2SO_4$ and $CaCO_3$. It was considered from the stoichiometric relationship that $SO_4^{2-}$ was in the form of $(NH_4)_2SO_4$ (Wang et al., 2005; Suzuki et al., 2008). $CaCO_3$ did not react with $SO_4^{2-}$ from polluted air. This is possible only when $CaCO_3$ does not mix with $SO_4^{2-}$ until all the $SO_4^{2-}$ is neutralized by $NH_4^+$ ('after' mixing). Mori et al. (1998) reported that $CaCO_3$ mixed with $(NH_4)_2SO_4$ did not convert to sulfate for a considerable period of time even at room temperature (23 °C), which gives a good basis for the preservation of the external mixture of $CaCO_3$ and $(NH_4)_2SO_4$ at a temperature as low as several degrees in centigrade at the summit of Mt. Fuji.

### 3.3. *The 'after' mixing index (AMI)*

In order to discuss the reason for the occurrence of the mixture of neutralized $SO_4^{2-}$ ($(NH_4)_2SO_4$) and unreacted $CaCO_3$ in the 'after' mixing, we have at first quantified the chemistry of the aerosols by introducing the 'after' mixing index (AMI). The triangle diagram in Fig. 4 can be trimmed into the triangle enclosed by lines 1, 2 and 3. The new triangle is now considered to be a mixing plane of three end-members: $CaCO_3$, $CaSO_4$ and $(NH_4)_2SO_4$. The outsides of the plane correspond to the acidic plane where $SO_4^{2-}$ is in excess over the sum of $Ca^{2+}$ and $NH_4^+$ (the left of Line 1) and to the $NH_4^+$ excess plane (the right of Line 2). Note that most of the data are plotted

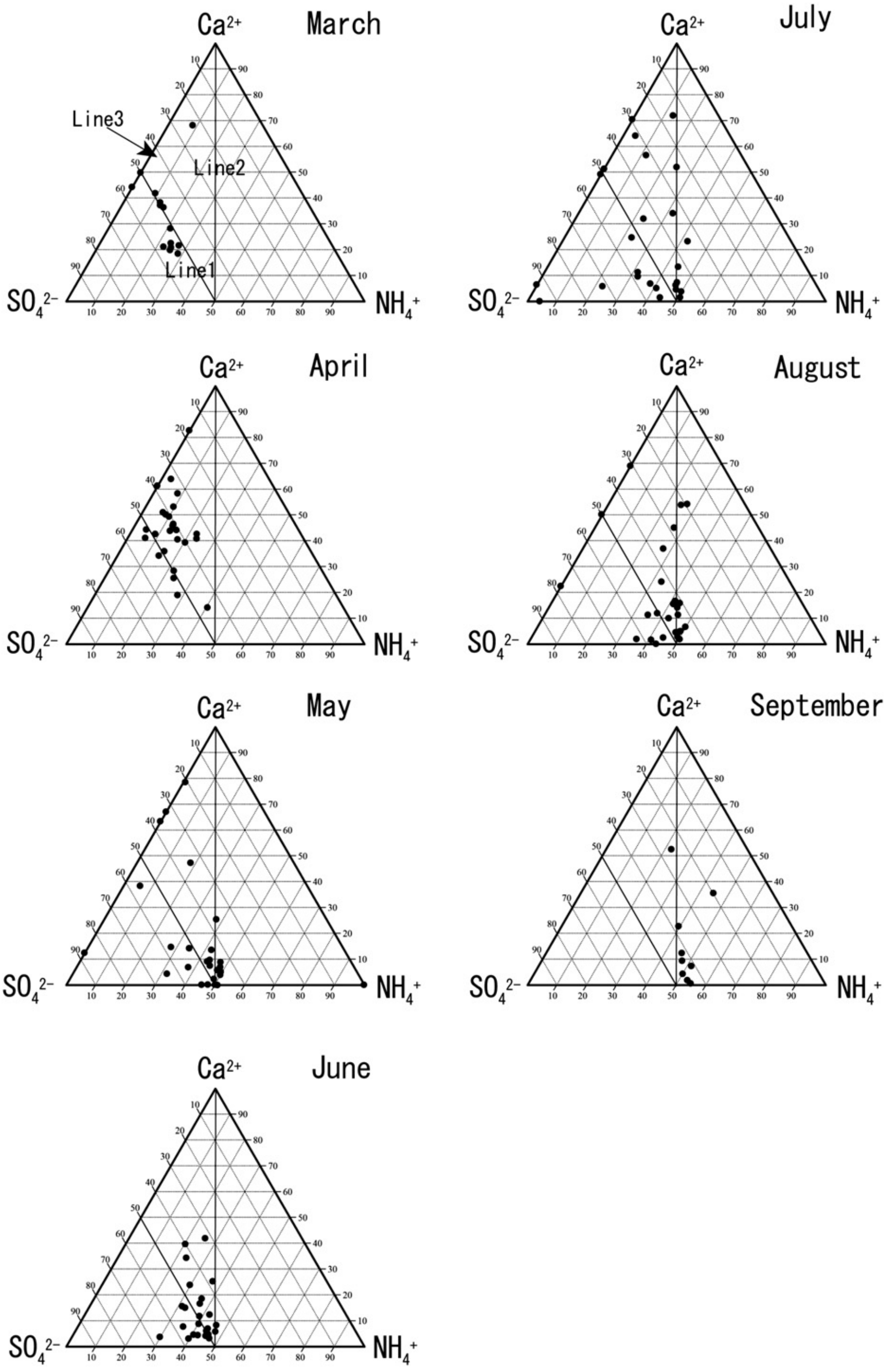

**Fig. 5.** Monthly triangle diagram ($Ca^{2+}$–$SO_4^{2-}$–$NH_4^+$) of aerosols at the summit of Mt. Fuji.

inside or near the new triangle of $CaCO_3$, $CaSO_4$ and $(NH_4)_2SO_4$, implying that the chemistry of the aerosols is largely described by the three end-members, as mentioned in the earlier discussion.

Now let us convert the tilted triangle into an equilateral triangle with the apexes corresponding to the three assumed end-members: $CaCO_3$, $CaSO_4$ and $(NH_4)_2SO_4$ (Fig. 6, right). Lines 1, 2 and 3 in Figs. 4 and6 (left) correspond to lines 1′, 2′ and 3′ in Fig. 6 (right), respectively. The base side (Line 2′), $CaCO_3$–$(NH_4)_2SO_4$, of the triangle corresponds to a mixture of neutralized $SO_4^{2-}$ and unreacted $CaCO_3$ (the situation corresponding to the 'after' mixing), and when $CaCO_3$ reacts with $SO_4^{2-}$ to form $CaSO_4$, the data points are located away from the base side in the triangle and approach either Line 1′ or Line 3′ (the situation corresponding to 'on-the-way' mixing). To weigh plots near Line 2′ more and plots close to Line 1′ or 3′ less, we have introduced the after mixing index (AMI). Let the proximity to each line be the reciprocal of the distance from the line. The relative proximity to the Line 2′ is now defined as the after mixing index (AMI), i.e.

$$\mathrm{AMI} = (1/d2')/(1/d1' + 1/d3' + 1/d2'),$$

where $d1'$, $d2'$ and $d3'$ are distances from the sides, Line 1′, Line 2′ and Line 3′, respectively. AMI is simply the proportion of the proximity to Line 2′ to the sum of proximities to all the three lines.

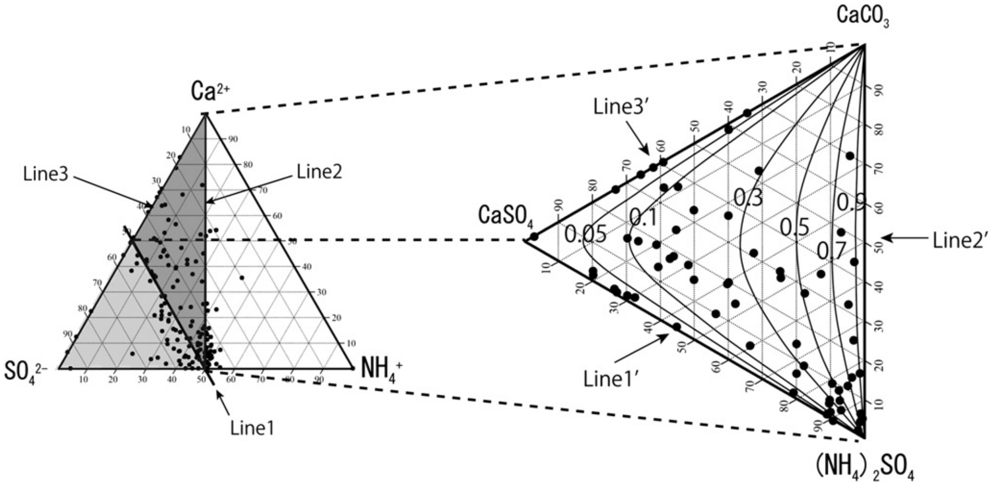

**Fig. 6.** ‘After’ mixing index (AMI) of the aerosols in the triangle diagram ($(NH_4)_2SO_4$–$CaCO_3$–$CaSO_4$) together with the data observed at the summit of Mt. Fuji.

The numeric formula of AMI is

$$AMI = \frac{\left(\frac{1}{2S-2N}\right)}{\left(\frac{1}{1-2S}+\frac{1}{2S-2N}+\frac{1}{2N}\right)},$$

where $S = SO_4^{2-}/(Ca^{2+} + SO_4^{2-} + NH_4^+)$, and $N = NH_4^+/(Ca^{2+} + SO_4^{2-} + NH_4^+)$.

The contours of the AMI values are drawn in Fig. 6 (right). The histogram exhibiting the frequency of the AMI values is shown in Fig. 7. The number of days having the AMI values greater than 0.7 was 10 during the four months from June to September (Table 1), whereas most of the data points were located in the region having AMI $< 0.3$ in March and April and no data during these two months is plotted in the region of AMI $> 0.7$. The mixture of unreacted $CaCO_3$ and $NH_3$-neutralized $SO_4^{2-}$ was typically seen in summer.

To understand the “after-mixing”, a new question “where does $SO_4^{2-}$ react with $NH_4^+$?” has to be answered. The intensity of ammonia emission is higher in summer than spring (Johnson et al., 2008). It is possible for $SO_4^{2-}$ to be neutralized with $NH_4^+$ around the sources of $SO_4^{2-}$. To consider the possibility, we examined the reported data on aerosols collected during summer in China and in an island in the Japan Sea. In aerosols collected in Shanghai, acid species ($SO_4^{2-} + NO_3^-$) was highly associated with $NH_4^+$ but they were incompletely neutralized by $NH_3$ (Yao et al., 2002). Pathak et al. (2008) collected aerosol samples in Beijing and Shanghai during summer season. They showed that $NH_4^+/SO_4^{2-}$ equivalent ratios were lower than unity (in Beijin 0.52, in Shanghai 0.69) and aerosols were not fully neutralized during summer. Geng et al. (2009) collected aerosol samples during June at Tokchok Island, Korea and identified $H_2SO_4$, $NH_4HSO_4$, $(NH_4)_2SO_4$ and carbonaceous matter using EPMA. The back trajectory analysis suggested that the aerosols were from China and Korea. Shimohara et al. (1999) performed sampling during July in Goto Island located in the Japan Sea and reported that average $H^+$ concentration in aerosol was 24 neq $m^{-3}$. Therefore, it is likely that $SO_4^{2-}$ has not been fully neutralized near the sources in summer and that the concentrations of $SO_4^{2-}$ exceed that of $NH_4^+$ in aerosols.

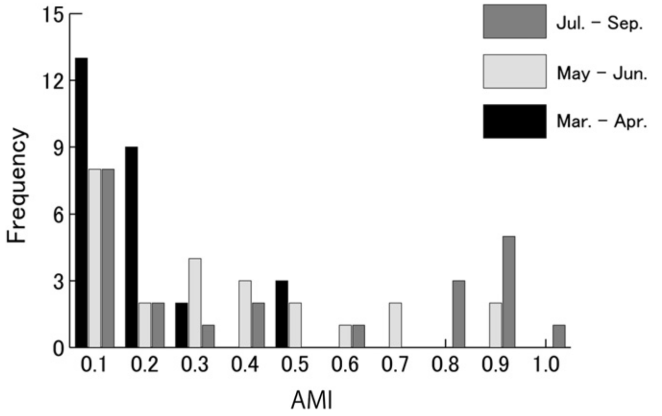

**Fig. 7.** The frequency of AMI values over different months.

Hatakeyama et al. (2004) reported that a large amount of $SO_4^{2-}$ was almost fully neutralized with $NH_4^+$ for the aerosols with a low concentration of $Ca^{2+}$ even during spring over the East China Sea. In our observation, the concentration range of $NH_4^+$ was 3.2–107.9 neq $m^{-3}$ for the “after-mixing” cases (Table 1), which were not always markedly higher than the range observed on normal Kosa days. In fact we observed an $NH_4^+$ concentration as high as 40–50 neq $m^{-3}$ on 4 days. In this case, the concentration of $SO_4^{2-}$ ranged from 80.8 to 107.4 neq $m^{-}$ and was in excess over that of $NH_4^+$ and $Ca^{2+}$ (30.4–53.6 neq $m^{-}$) are considered to have interfered with the neutralization reaction between $SO_4^{2-}$ and $NH_4^+$ in spring.

From the line of evidences we consider that the high emission of ammonia is not necessarily the cause of the ‘after-mixing’ events, although the possibility is not entirely excluded. We then explored the possibility of difference in transportation routes of sulfate aerosols and Kosa particles in the follow section.

**Table 1**
The list of the days whose AMI[a] values are greater than 0.7.

| Day | $Ca^{2+}$ (neq $m^{-3}$) | $NH_4^+$ (neq $m^{-3}$) | $SO_4^{2-}$ (neq $m^{-3}$) | AMI |
|---|---|---|---|---|
| 2002/6/9 | 8.7 | 12.7 | 13.2 | 0.85 |
| 2002/7/3 | 163.4 | 29.6 | 34.4 | 0.82 |
| 2002/7/16 | 10.6 | 107.9 | 108.7 | 0.84 |
| 2002/7/24 | 8.1 | 7.5 | 8.1 | 0.82 |
| 2002/7/31 | 8.4 | 62.9 | 63.5 | 0.85 |
| 2002/8/2 | 30.5 | 81.0 | 84.5 | 0.77 |
| 2002/8/4 | 8.2 | 87.6 | 88.6 | 0.78 |
| 2002/8/20 | 16.7 | 9.9 | 10.5 | 0.89 |
| 2002/8/21 | 7.3 | 18.0 | 18.3 | 0.91 |
| 2002/9/1 | 7.6 | 3.2 | 3.7 | 0.78 |

[a] AMI: “after” mixing index (see 3.3).

### 3.4. *Trajectory analysis for air having AMI $< 0.3$ and $Ca^{2+}$ concentration greater than the annual mean concentration of $Ca^{2+}$ (the case of 'on-the-way' mixing)*

To examine the transport route of Kosa particles, we calculated the trajectories for the days where the $Ca^{2+}$ concentration was greater than the average concentrations of $Ca^{2+}$ (9.3 nmol $m^{-3}$) from the middle of March till the beginning of September and having an AMI $< 0.3$ with METEX at the heights of 1500, 2500, 3800, 5000 and 7000 m at the geographical point of Mt. Fuji (Fig. 8). For the days, the routes of air at the heights of 1500, 2500, 3800, 5000 and 7000 m were more or less similar to each other, and almost all of them were from central Asia. This air mass was transported through industrial areas in China, and was likely mixed with the polluted air mass on the way to Mt. Fuji ('on-the-way' mixing). Therefore, most of the $Ca^{2+}$ in $CaCO_3$ was converted to $CaSO_4$ because of the chemical reaction between $SO_4^{2-}$ and $CaCO_3$ within the Kosa particles (Suzuki et al., 2008; Wang et al., 2005).

### 3.5. *Trajectory of the summer air mass (the case of 'after' mixing)*

AMI values which are greater than 0.7 were only seen in summer (Fig. 7). In other words, unreacted $CaCO_3$ mixed with $SO_4^{2-}$ from $(NH_4)_2SO_4$ in aerosols was only seen in summer. Therefore, the transport mechanisms of aerosols with each of the AMI values were examined in summer. The back trajectories from the geographical point of Mt. Fuji calculated with METEX for the air having AMI values less than 0.3 and greater than 0.7 during summer from July to September are separately shown in Fig. 9. The altitudes from which the calculation started were 1500, 2500, 3800, 5000 and 7000 m.

Most of the air masses having AMI $< 0.3$ came almost exclusively from the Pacific Ocean for any altitudes from the lower layer to the upper layer, and some of the air in the upper layer (7000 m) was from Central Asia (Fig. 9, right). In summer, the marine air mass expanded over Japan because of high pressures over the Pacific Ocean during the season. Most of the 5000 and 7000 m air masses having AMI $> 0.7$ were transported over desert area near the Tarim basin, and those of 3800 m were transported mainly over China. However, almost all of the air measured at 1500 and 2500 m was transported mainly from the Pacific Ocean, similar to the case of air having AMI $< 0.3$. The results of back trajectories of the lower air masses for the case of AMI $> 0.7$ are correlated closely with the concentrations of $SO_4^{2-}$ and $NH_4^+$ in the aerosols. For the air masses with high concentrations of $SO_4^{2-}$ and $NH_4^+$ (e.g. July 16th, August 2nd and 4th, marked * in Fig. 9, left), the 1500–3800 m air masses were transported from the areas around Yellow Sea and Korean Peninsula. For the air masses with the lower concentrations of the ions (e.g. July 3rd, marked + in Fig. 9, left), the air masses in the lower layers were transported from the Pacific Ocean. Regardless of the concentrations of $SO_4^{2-}$ and $NH_4^+$, the air masses in the upper layer were transported from central Asia. Therefore, it was considered that the Kosa-representative element, Ca, in the aerosols was transported only through the upper troposphere in the case of AMI $> 0.7$.

Matsuki et al. (2003) performed back trajectory analysis and reported that the dust particles were transported from the Tarim basin to Japan through the middle free troposphere (>4 km) in summer.

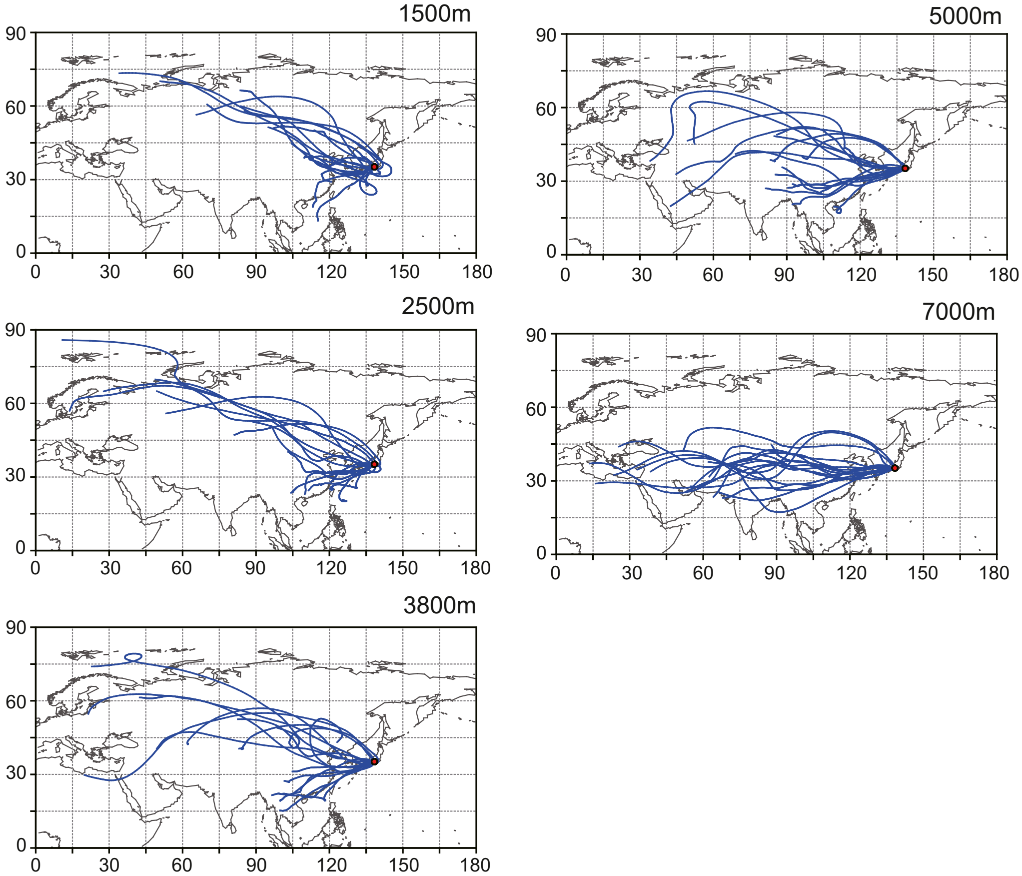

**Fig. 8.** Back trajectory of the air masses of AMI $< 0.3$ and $Ca^{2+}$ greater than the average concentration during the middle of March to the beginning of September (9.3 nmol $m^{-3}$) at different altitudes. Trajectories for the preceding 120 h were calculated.

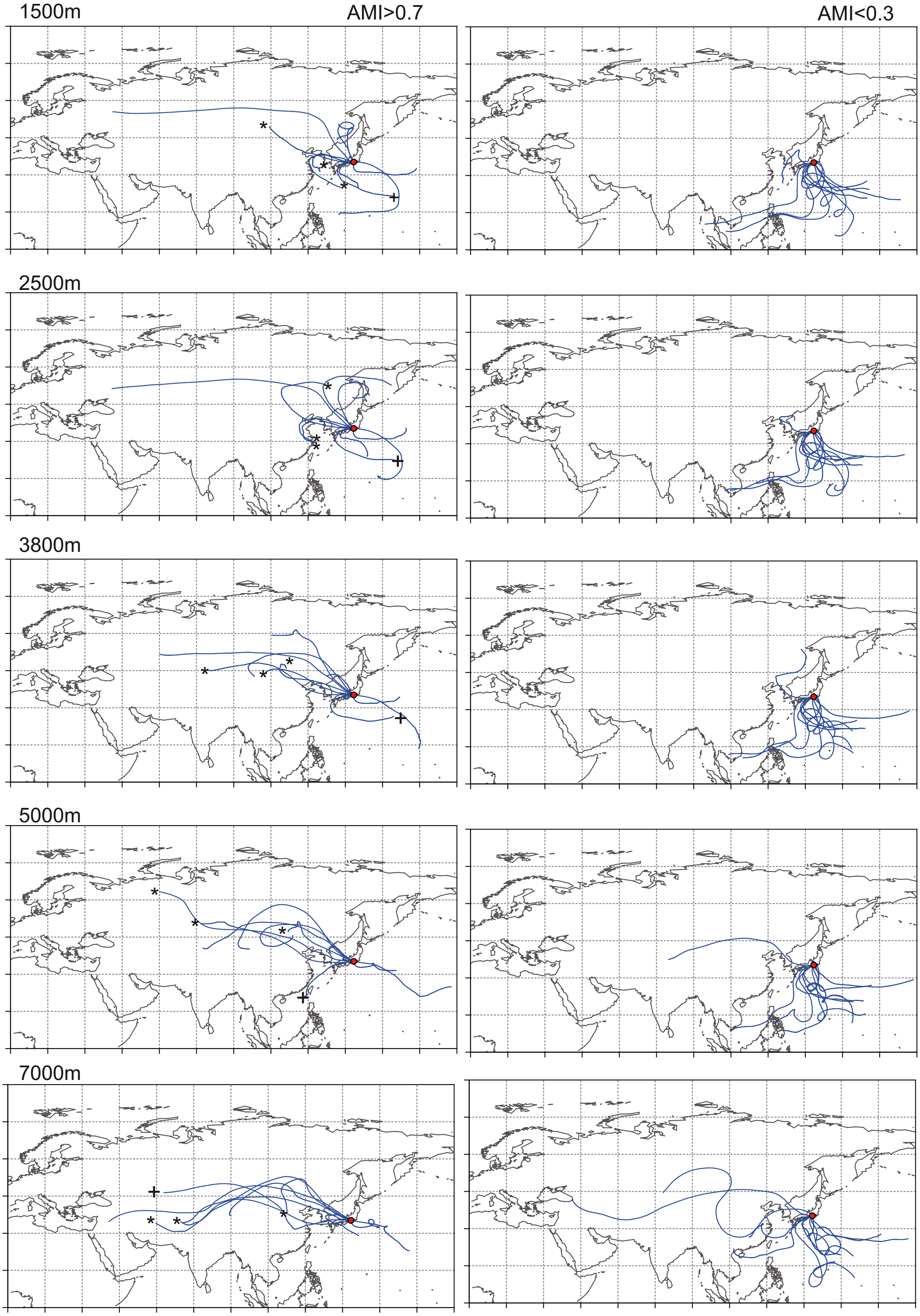

**Fig. 9.** Back trajectory of air masses during the summer (July–September) at different altitudes. Trajectories for the preceding 120 h were calculated. Trajectories marked with * are for July 16th, August 2nd and 4th, where high concentrations of $SO_4^{2-}$ and $NH_4^+$ were observed and that marked with + is for the case of the low concentrations of the ions (July 3rd).

The particles have soared up the middle free troposphere by a strong thermal plume in the surrounding mountains, which is most active in summer, and they are then carried by the westerly jet. They named this phenomenon 'background Kosa' to discern it from normal Kosa. Huang et al. (2007) observed dust layers most frequently at altitudes of around 4–7 km using the CALIPSO satellite. They also suggested that dust from the Taklamakan Desert was entrained to an elevation of 5 km or higher and that they were then transported over the Tibetan plateau by the low thermal cyclone. Therefore, it was considered that $CaCO_3$ was lifted up by a thermal plume and/or by a low thermal cyclone and was then transported through the middle troposphere by circumpolar westerlies.

During the background Kosa episodes, almost no Kosa particles were observed at low-lying observatories. Anthropogenically or naturally produced $SO_4^{2-}$ ions are somehow neutralized by rather ubiquitous ammonia or ammonium (Johnson et al., 2008) to produce $(NH_4)_2SO_4$, which becomes a typical component of aerosols in the low layer (Hatakeyama et al., 2004; Fu et al., 2004).

Aerosols of $CaCO_3$ in the upper layer air and well-neutralized $(NH_4)_2SO_4$ in the lower layer were 'after' mixed just prior to beinge sampled. When $SO_4^{2-}$ in the lower layer has completely reacted with $NH_4^+$ on the way to Mt. Fuji, $CaSO_4$ might not have been produced by the reaction between $CaCO_3$ and $SO_4^{2-}$ ('after' mixing). According to the back trajectory analysis, the lower air mass and the upper air mass have no opportunity to mix together. $(NH_4)_2SO_4$ exists as fine particles, and $CaCO_3$ exists as coarse particles (Kim and Park, 2001); therefore, the terminal settling velocity of $CaCO_3$ is much higher than that of $(NH_4)_2SO_4$. It is expressed using Stokes' formula as follows:

$$v_s = \frac{2(\rho_p - \rho_a)}{9\mu} a^2 g, \tag{1}$$

where $\rho_p$ is the particle density ($CaCO_3$: 2700 kg $m^{-3}$), $\rho_a$ is the air density (1.2 kg $m^{-3}$), $a$ is the diameter of the particle and $\mu$ is the viscosity of air (0.000018 Pa s).

The vertical settling distance of particles per day are calculated as 7.1 m for the diameter 1 μm, 28 m for the 2 μm, 180 m for the 5 μm and 710 m for the 10 μm particles. The results of back trajectory analysis (Fig. 9) indicated that it took 4–5 days for the air mass to fly from the Tarim basin to Mt. Fuji. If the particles were assumed to start their journey at an altitude of 4000–6000 m, particles having 1–5 μm diameters were considered to be transported to the summit of Mt. Fuji. Relatively coarser particles were transported to the summit of Mt. Fuji, settling from the mid free troposphere, which caused 'after' mixing. Transport in not only the horizontal but also the vertical direction needs to be considered.

## 4. Conclusion

The present study has disclosed the occurrence of two discreet chemistries of the atmospheric aerosols, which is caused by the different order of mixing of materials supplied from the ground: $H_2SO_4$ and calcium carbonate. If the two species mix early, they react with each other, resulting in sulfate ions and the reacted form of $CaSO_4$. If the two mix late, $H_2SO_4$ absorbs $NH_4^+$ ions and becomes inactive before they meet. The two types of mixing are clearly demonstrated by our semi-continuous observation at the summit of Mt. Fuji over the course of different seasons. 'On-the-way' mixing occurs in spring, and 'after' mixing occurs exclusively in summer. This explains the observed change in the $NH_4^+/SO_4^{2-}$ ratio (Fig. 2).

The difference in aerosol chemistry may affect further phases of the Earth's environment. Even if the mixing ratio of the two components is the same, the behaviour of sulfate ions and ammonia would be greatly affected by the order of mixing. In the case of 'on-the-way' mixing, sulfate is bound to relatively large particles supplied from deserts, and ammonia would remain as a gaseous species in the atmosphere whereas in the case of 'after' mixing, sulfate and ammonia form very fine particles of ammonium sulfate, which remain suspended in the atmosphere longer and act as condensation nuclei for clouds. The methods of mixing would affect the climate as well as the activity of biota. The present study provides basic information on the qualitative aspect of this mixing, and we hope to report the quantitative analysis in the future.

## Acknowledgements

We would like to express our gratitude to the staff of Mt. Fuji Weather Station for performing the sampling.

## Reference

Berresheim, H., Andreae, M.O., Ayers, G.P., Gillett, R.W., Merrill, J.T., Davis, V.J., Chameides, W.L., 1990. Airborne measurements of Dimethylsulfide, sulfur dioxide, and aerosol ions over the southern ocean South of Australia. Journal of Atmospheric Chemistry 10, 341–370.

Chang, Q., Mishima, T., Yabuki, S., Takahashi, Y., Shimizu, H., 2000. Sr and Nd isotope ratios and REE abundances of moraines in the mountain areas surrounding the Taklimakan Desert, NW China. Geochemical Journal 34, 407–427.

Fu, F.-F., Watanabe, K., Yabuki, S., Akagi, T., 2004. Seasonal characteristics of chemical compositions of the atmospheric aerosols collected in urban seaside area at Tokaimura, eastern central Japan. Journal of Geophysical Research 109 (D20212), 1–9.

Geng, H., Jung, H.J., Park, Y.M., Hwang, H.J., Kim, H.K., Kim, Y.J., Sunwoo, Y., Ro, C.U., 2009. Morphological and chemical composition characteristics of summertime atmospheric particles collected at Tokchok Island, Korea, Atmospheric Environment 43, 3364–3373.

Hatakeyama, S., Takami, A., Sakamaki, F., Mukai, H., Sugimoto, N., Shimizu, A., Bandow, H., 2004. Aerial measurement of air pollutants and aerosols during 20–22 March 2001 over the East China Sea. Journal of Geophysical Research 109 (D13304). doi:10.1029/2003JD004271.

Huang, J., Minnis, P., Yi, Y., Tang, Q., Wang, X., Hu, Y., Liu, Z., Ayers, K., Trepte, C., Winker, D., 2007. Summer dust aerosols detected from CALIPSO over the Tibetan Plateau. Geophysical Research Letter 34 (L18805). doi:10.1029/2007GL029938.

Ito, T., Okita, T., Ikegami, M., Kanazawa, I., 1986. The characterization and distribution of aerosol and gaseous species in the winter monsoon over the western pacific ocean. Journal of Atmospheric Chemistry 4, 401–411.

Iwasaka, Y., Yamato, M., Imasu, R., Ono, A., 1988. Transport of Asian dust (KOSA) particles: importance of weak KOSA envents on the geochemical cycle of soil particles. Tellus 40B, 494–503.

Iwasaka, Y., et al., 2003. Large depolarization ratio of free tropospheric aerosols over the Taklamakan Desert revealed by lidar measurements: possible diffusion and transport of dust particles. Journal of Geophysical Research 108 (D23), 8652. doi:10.1029/2002JD003267.

Iwasaka, Y., Shi, G.-Y., Kim, Y.S., Matsuki, A., Trochkine, D., Zhang, D., Yamada, M., Nagatani, T., Nagatani, M., Shen, Z., Shibata, T., Nakata, H., 2004. Pool of dust particles over the Asian continent: balloon-borne optical particle counter and ground-based lidar measurements at Dunhuang, China. Environmental Monitoring and Assessment 92, 5–24.

Johnson, M.T., Liss, P.S., Bell, T.G., Lesworth, T.J., Baker, A.R., Hind, A.J., Jickells, T.D., Biswas, K.F., Woodward, E.M.S., Gibb, S.W., 2008. Field observations of the ocean-atmosphere exchange of ammonia: fundamental importance of temperature as revealed by a comparison of high and low latitudes. Global Biogeochemical Cycles 22 (GB1019). doi:10.1029/2007GB003039.

Kai, K., Okada, Y., Uchino, O., Tabata, I., Nakamura, H., 1988. Lidar observation and numerical simulation of a Kosa (Asian dust) over Tsukuba, Japan during the spring of 1986. Meteorological Society of Japan, Journal 66, 457–472.

Kim, B., Park, S., 2001. Transport and evolution of a winter-time Yellow sand observed in Korea. Atmospheric Environment 35, 3191–3201.

Kim, Y.S., Iwasaka, Y., Shi, G.-Y., Nagatani, T., Shbata, T., Trochkine, D., Matsuki, A., Yamada, M., Chen, B., Zhang, D., Nagatani, M., Nakata, H., 2004. Dust particles in the free atmosphere over Deseart areas on the Asian continent: measurements from summer 2001 to summer 2002 with balloon-borne optical particle counter and lidar, Dunhuang, China. Journal of Geophysical Research 109, D19S26. doi:10.1029/2002JD003269.

Li, L., Chen, Z.M., Zhang, Y.H., Zhu, T., Li, J.L., Ding, J., 2006. Kinetics and mechanism of heterogeneous oxidation of sulfur dioxide by ozone on surface of calcium carbonate. Atmospheric Chemistry and Physics 6, 579–613.

Matsuki, A., Iwasaka, Y., Osada, K., Matsunaga, K., Kido, M., Inomoto, Y., Trochkine, D., Nishita, C., Nezuka, T., Sakai, T., Zhang, D., Kwon, S.A., 2003. Seasonal dependence of the long-range transport and vertical distribution of free tropospheric aerosols over east Asia: on the basis of aircraft and lidar measurements and isentropic trajectory analysis. Journal of Geophysical Research 108 (D23), 8663. doi:10.1029/2002JD003266.

Mori, I., Nishikawa, M., Iwasaka, Y., 1998. Chemical reaction during the coagulation of ammonium sulphate and mineral particles in the atmosphere. The Science of the Total Environment 224, 87–91.

Nishikawa, M., Kanamori, S., Kanamori, N., Mizoguchi, T., 1991. Kosa aerosol as eolian carrier of anthropogenic material. The Science of the Total Environment 107, 13–27.

Okada, K., Kai, K., 1995. Features and elemental composition of mineral particles collected in Zhangye, China. Journal of the Meteorological Society of Japan 73, 959–965.

Okada, K., Qin, Y., Kai, K., 2005. Elemental composition and mixing properties of atmospheric mineral particles collected in Hohhot, China. Atmospheric Research 73, 45–67.

Pathak, R.K., Wu, W.S., Wang, T., 2008. Summertime PM2.5 ionic species in four major cities of China: nitrate formation in an ammonia-deficient atmosphere. Atmospheric Chemistry and Physics Discussions 8, 11487–11517.

Sakai, T., Shibata, T., Iwasaka, Y., Nagai, T., Nakazato, M., Matsumura, T., Ichiki, A., Kim, Y.-S., Tamura, K., Troshkin, D., Hamdi, S., 2002. Case study of Raman lidar measurements of Asian dust events in 2000 and 2001 at Nagoya and Tsukuba, Japan. Atmospheric Evironment 36, 5479–5489.

Shimohara, T., Oishi, O., Utsunomiya, A., Sakurai, T., Niiya, S., Kamaya, T., Mukai, H., Hatakeyma, S., Murano, K., 1999. Properties of gases and particulate matters at two sites of northern Kyushu in Japan: origin of acidic substances and acidification factors in summer and winter seasons. In: Proceeding of the 40th Annual Meeting of the Japan Society for Atmospheric Environment 1999, 583 (in Japanese).

Suzuki, I., Hayashi, K., Igarashi, Y., Takahashi, H., Sawa, Y., Ogura, N., Akagi, T., Dokiya, Y., 2008. Seasonal variation of water-soluble ion species in the atmospheric aerosols at the summit of Mt. Fuji. Atmospheric Environment 42, 8027–8035.

Takemura, T., Uno, I., Nakajima, T., Higurashi, A., Sano, I., 2002. Modeling study of long-range transport of Asian dust and anthropogenic aerosols from East Asia. Geophysical Research Letters 29 (24), 2158. doi:10.1029/2002GL016251.

Tanaka, T.Y., Kurosaki, Y., Chiba, M., Matsumura, T., Nagai, T., Yamazaki, A., Uchiyama, A., Tsunematsu, N., Kai, K., 2005. Possible transcontinental dust transport from north Africa and the middle east to east Asia. Atmospheric Environment 39, 3901–3909.

Tsai, Y.I., Chen, C., 2006. Characterization of Asian dust storm and non-Asian dust storm PM2.5 aerosol in southern Taiwan. Atmospheric Environment 40, 4734–4750.

Wang, Y., Zhuang, G., Sun, Y., An, Z., 2005. Water-soluble part of the aerosol in the dust storm season-evidence of the mixing between mineral and pollution aerosols. Atmospheric Environment 39, 7020–7029.

Watanabe, K., 2005. Influence of background Kosa on chemical compositions in fog water at a Mountainous site. Tenki (in Japanese) 52, 533–538.

Yabuki, S., Kanayama, S., Fu, F., Honda, M., Yanagisawa, F., Wei, W., Zheng, F., Liu, M., Shen, Z., Liu, L., 2002. Physical and chemical characteristics of aeolian dust collected over Asian dust source regions in China-comparison with atmospheric aerosols in an urban area at Wako, Japan. Journal of Arid Land Studies 11, 273–289.

Yao, X., Chan, C.K., Fang, M., Cadle, S., Chan, T., Mulawa, P., He, K., Ye, B., 2002. The water-soluble ionic composition of PM2.5 in Shanghai and Beijing, China. Atmospheric Environment 36, 4223–4234.

Yuan, H., Zhuang, G., Rahn, K.A., Zhang, X., Li, Y., 2006. Composition and mixing of individual particles in dust and nondust conditions of north China, spring 2002. Journal of Geophysical Research 111 (D20208). doi:10.1029/2005JD006478.

Zeng, J., Tohjima, Y., Fujinuma, Y., Mukai, H., Katsumoto, M., 2003. A study of trajectory quality using methane measurements from Hateruma Island. Atmospheric Environment 37, 1911–1919.